J Physiol 588.17 (2010) pp 3255–3266

The Journal of Physiology

Interaction with caveolin-1 modulates vascular ATP-sensitive potassium (K_{ATP}) channel activity

Lowri M. Davies[1], Gregor I. Purves[1], Richard Barrett-Jolley[2] and Caroline Dart[1]

[1] *Biosciences Building, School of Biological Sciences, University of Liverpool, Crown Street, Liverpool L69 7ZB, UK*
[2] *Department of Veterinary Preclinical Science, University of Liverpool, Brownlow Hill, Liverpool L69 7ZY, UK*

ATP-sensitive potassium channels (K_{ATP} channels) of arterial smooth muscle are important regulators of arterial tone, and hence blood flow, in response to vasoactive transmitters. Recent biochemical and electron microscopic evidence suggests that these channels localise to small vesicular invaginations of the plasma membrane, known as caveolae, and interact with the caveolae-associated protein, caveolin. Here we report that interaction with caveolin functionally regulates the activity of the vascular subtype of K_{ATP} channel, Kir6.1/SUR2B. Pinacidil-evoked recombinant whole-cell Kir6.1/SUR2B currents recorded in HEK293 cells stably expressing caveolin-1 (69.6 ± 8.3 pA pF^{-1}, $n = 8$) were found to be significantly smaller than currents recorded in caveolin-null cells (179.7 ± 35.9 pA pF^{-1}, $n = 6$; $P < 0.05$) indicating that interaction with caveolin may inhibit channel activity. Inclusion in the pipette-filling solution of a peptide corresponding to the scaffolding domain of caveolin-1 had a similar inhibitory effect on whole-cell Kir6.1/SUR2B currents as co-expression with full-length caveolin-1, while a scrambled version of the same peptide had no effect. Interestingly, intracellular dialysis of vascular smooth muscle cells with the caveolin-1 scaffolding domain peptide (SDP) also caused inhibition of pinacidil-evoked native whole-cell K_{ATP} currents, indicating that a significant proportion of vascular K_{ATP} channels are susceptible to block by exogenously applied SDP. In cell-attached recordings of Kir6.1/SUR2B single channel activity, the presence of caveolin-1 significantly reduced channel open probability (from 0.05 ± 0.01 to 0.005 ± 0.001; $P < 0.05$) and the amount of time spent in a relatively long-lived open state. These changes in kinetic behaviour can be explained by a caveolin-induced shift in the channel's sensitivity to its physiological regulator MgADP. Our findings thus suggest that interaction with caveolin-1 suppresses vascular-type K_{ATP} channel activity. Since caveolin expression is regulated by cellular free cholesterol and plasma levels of low-density lipoprotein (LDL), this interaction may have implications in both the physiological and pathophysiological control of vascular function.

(Received 14 June 2010; accepted after revision 8 July 2010; first published online 12 July 2010)
Corresponding author C. Dart: Biosciences Building, School of Biological Sciences, University of Liverpool, Crown Street, Liverpool L69 7ZB, UK. Email: c.dart@liv.ac.uk

Abbreviations CSD, caveolin scaffolding domain; LDL, low-density lipoprotein; LL, log-likelihood; PDFs, probability distribution functions; PKCε, protein kinase Cε; SDP, scaffolding domain peptide; SKM, segmental K mean; SUR, sulphonylurea receptor.

Introduction

Caveolae are stable, flask-shaped pits (60–80 nm in diameter) that form at the plasma membrane of most cells when tightly-packed aggregates of cholesterol and sphingolipids associate with the cholesterol-binding protein caveolin (Anderson, 1998; Galbiati *et al.* 2001; Razani *et al.* 2002; Parton & Simons, 2007). Varied physiological roles have been assigned to these structures including vesicular transport, control of cellular cholesterol, T-tubule development, and mechano-transduction (Razani *et al.* 2002; Parton & Simons, 2007). In addition, the apparent ability of caveolae to selectively recruit interacting signalling molecules, including G protein-coupled receptors, G proteins, protein kinases and various classes of ion channel, has led to the idea that they act as subcellular compartments for the initiation or modulation of signalling events (Razani *et al.* 2002; Parton & Simons, 2007; Patel *et al.* 2008). Aside from roles in caveolae formation and stability, caveolins also

DOI: 10.1113/jphysiol.2010.194779

interact with many caveolae-localized signalling molecules (Razani *et al.* 2002; Patel *et al.* 2008). Interaction occurs via a 20 amino acid N-terminal region on the caveolin molecule known as the caveolin scaffolding domain (CSD) and typically suppresses activity in the associated protein (Couet *et al.* 1997; Okamoto *et al.* 1998).

One of the many signalling proteins that have been shown to reside in caveolae and interact with caveolins is the vascular subtype of ATP-sensitive potassium (K_{ATP}) channel (Sampson *et al.* 2004, 2007; Jiao *et al.* 2008). These channels form as heterooctamers of four Kir6 pore-forming subunits and four regulatory sulphonylurea receptor (SUR) subunits (Aguilar-Bryan *et al.* 1998), with the dominant channel in vascular smooth muscle most likely comprising Kir6.1/SUR2B (Chutkow *et al.* 2002; Miki *et al.* 2002; Cole & Clement-Chomienne, 2003). Vascular K_{ATP} channels have been described in smooth muscle cells from a variety of arterial beds where they provide a background K^+ conductance important in the regulation of membrane potential and thus smooth muscle contractility and blood flow (Quayle *et al.* 1997; Clapp & Tinker, 1998; Yokoshiki *et al.* 1998; Cole & Clement-Chomienne, 2003). Garg *et al.* (2009*a*,*b*) have recently demonstrated a role for caveolin in the regulation of cardiac K_{ATP} channel activity, but despite the potential importance of understanding how vascular channels are regulated in both normal and disease states, little is known about the role of caveolae or caveolins in controlling vascular K_{ATP} channel function.

Our previous work has shown that vascular K_{ATP} channels localize to the same cholesterol-enriched smooth muscle membrane fractions as the caveolae marker, caveolin (Sampson *et al.* 2004, 2007). We have also shown in immunogold electron micrographs of rat aortic smooth muscle plasma membrane sheets that vascular K_{ATP} channel subunits are present in morphologically identifiable regions of the membrane rich in caveolin (Sampson *et al.* 2007). Additionally, antibodies against the Kir6.1 subunit of the channel coimmunoprecipitate caveolins from rat aortic homogenates, suggesting these proteins form part of a complex (Sampson *et al.* 2004). Here we compare the kinetic behaviour of recombinant vascular K_{ATP} channels in the presence and absence of caveolin to assess the functional effect of association with caveolin on channel activity.

Methods

Cells and cell transfection

HEK293 cells were grown as previously described (Leyland & Dart, 2004) in minimum essential medium (MEM) containing GlutaMAX, 10% fetal bovine serum, 1% MEM non-essential amino acids, penicillin (50 U ml^{-1}) and streptomycin (50 U ml^{-1}) in a 5% CO_2 humidified atmosphere at 37°C. All media and reagents were from Invitrogen. HEK293 cells stably expressing caveolin-1 were grown under the same conditions with the addition of 0.5 mg ml^{-1} G418-disulphate (Melford Laboratories Ltd, Ipswich, UK) to the medium. Cells were transiently transfected with Kir6.1/SUR2B using Lipofectamine 2000 Transfection Reagent (Invitrogen) according to the manufacturer's protocol.

DNA constructs

pcDNA3-caveolin-1 was a gift from Dr Laura Sampson (University of Leicester, UK); pcDNA3-SUR2B was a gift from Prof. Yoshihisa Kurachi (Osaka University, Japan) and pIRES2-EGFP-Kir6.1 a gift from Prof. Susumu Seino (Kobe University, Japan). cDNAs for caveolin-1, Kir6.1 and SUR2B were prepared using a plasmid midi-kit (Qiagen) according to the manufacturer's instructions.

Animals

Tissues were obtained from adult male Wistar rats (175–200 g) (Charles River Laboratories, Inc. Margate, UK) which were killed by rising concentration of CO_2 followed by exsanguination. The care and killing of animals conformed to the requirements of the UK Animals (Scientific Procedures) Act 1986.

Smooth muscle cell isolation

Following dissection, the rat thoracic aorta was placed into chilled zero Ca^{2+} buffer containing (mM): 137 NaCl, 5.4 KCl, 0.4 NaH_2PO_4, 0.4 Na_2HP0_4, 1 $MgCl_2$, 10 Hepes, 10 glucose, pH 7.4. The aorta was cleaned of all connective tissue and cut transversely every 2–4 mm into rings which were then opened up to form strips. Single cells were obtained using an enzymatic digestion procedure. Arteries were incubated for 45 min at 35°C in a 0.1 mM Ca^{2+} buffer containing 1.4 mg ml^{-1} papain, 0.9 mg ml^{-1} dithioerythritol and 0.9 mgml-1 bovine serum albumin (all Sigma-Aldrich). The 0.1 mM Ca^{2+} buffer contained (mM): 137 NaCl, 5.4 KCl, 0.4 NaH_2PO_4, 0.4 Na_2HP0_4, 1 $MgCl_2$, 0.1 $CaCl_2$, 10 Hepes, 10 glucose, pH adjusted to 7.4 with NaOH. After enzyme treatment the artery was rinsed in 0.1 mM Ca^{2+} buffer, and single cells were dispersed in this solution by trituration of the tissue through a heat-polished Pasteur pipette.

Electrophysiology

HEK293 and HEK293 caveolin-1 cells were plated onto 12- or 24-well plates 24 h prior to transient transfection with cDNAs encoding Kir6.1 and SUR2B (1:1 cDNA ratio for transfection). Whole-cell, cell-attached or inside-out recordings of recombinantly expressed Kir6.1/SUR2B channels were made typically 24–48 h post-transfection

using an Axopatch 200B amplifier (Molecular Devices, Sunnyvale, CA, USA). Whole cell currents were also recorded from freshly dissociated single smooth muscle cells.

For single channel recordings, patch pipettes were pulled from borosilicate glass capillaries (outer diameter 1.5 mm, inner diameter 0.86 mm; Harvard Apparatus) and fire-polished to give a final resistance of 10–15 MΩ when filled. For cell-attached single-channel recordings, the bath solution contained (in mM): 140 KCl, 1 $MgCl_2$, 0.1 $CaCl_2$, 10 Hepes, 10 glucose, adjusted to pH 7.4. The pipette filling solution was as the bath solution. For inside-out single-channel recordings, the bath solution contained (in mM): 140 KCl, 2 $MgCl_2$, 5 EGTA, 5 Hepes, pH 7.3. The pipette filling solution for these experiments contained (in mM): 140 KCl, 1 $MgCl_2$, 1 $CaCl_2$, 5 Hepes, pH 7.4. Single-channel recordings were filtered at 2 kHz, sampled at 10 kHz using a Digidata 1320A interface (Molecular Devices), and analysed using pCLAMP (Molecular Devices) and QuB (Dr Feng Qin, Dr Lorin Milescu, Fu Qiong, Chris Nicolai and John Bannen, SUNY, Buffalo, NY, USA) software. Whole-cell K^+ currents were recorded as previously described (Sampson *et al.* 2004).

Caveolin scaffolding domain peptide, corresponding to amino acids 82–101 of caveolin-1 (DGIWKASFTTFTVTKYWFYR), and a scrambled version of the same peptide (GDAWKYRF-WTFTKSYTFTV) were synthesised by Sigma-Aldrich. Pinacidil and glibenclamide were purchased from Sigma-Aldrich. All experiments were performed at room temperature (18–22°C), and the results are expressed as the mean ± S.E.M. Statistical significance was evaluated using ANOVA followed by the Tukey–Kramer multicomparison test (StatsDirect, Altrincham, UK) except where stated.

Single channel model

Data were idealised with the segmental K means (SKM) methods (Qin, 2004) using QuB software. Models were fitted to the data by maximum interval likelihood optimisation to the SKM idealized record (Qin *et al.* 1996, 1997). Dead-time was set to three sample intervals. Several hundred possible model state schemes were searched and assessed by maximisation of log-likelihood (LL). States were added progressively until there was no longer a significant increase in LL/event. At this point model fitting was constrained to a maximum of eight connections and three exits per state in order to keep numerical computations practicable. The model returning the largest aggregate LL/event value was used to calculate rates and equilibrium occupancy values for each patch used. Bursts were defined as groups of openings separated by closure longer than a fixed critical time T_c. The critical time was in turn determined by equalising the areas of short events misclassified as long and long misclassified as short in the closed times probability distribution functions (PDFs). Equilibrium occupancy and transition rate hypothesis testing were performed with the SPSS General Linear Model (GLM) routine in SPSS 16.0 for Windows (SPSS Inc, Chicago, IL, USA).

Dose–response curve fitting

Pinacidil dose response curves were fitted as previously described (Barrett-Jolley *et al.* 1999). Data comparing the effects of differing nucleotide (ATP or ADP) concentrations on Kir6.1/SUR2B activity in caveolin-null and caveolin-1 expressing cells were fitted with a biphasic concentration effect curve in Origin (OriginLab Corp., Northampton, MA, USA) using:

$$f = f_{\max} \cdot \left([c]^{h_1}/\left([c]^{h_1} + K_{d1}^{h_1}\right)\right) \cdot \left(1 - \left([c]^{h_2}/\left([c]^{h_2} + K_{d2}^{h_2}\right)\right)\right) \quad (1)$$

where f is the fractional current remaining in the presence of nucleotide, $f_{\max}$ is the maximum current and $[c]$ the concentration of nucleotide. K_{d1}, h_1 and K_{d2}, h_2 are the midpoint and Hill coefficients for positive and inhibitory sites, respectively. Data are presented as means ± S.E.M. of fits to individual cell data. To achieve a good fit to individual cell data, h_1 and/or h_2 had to be constrained to unity in some cases. Statistical significance was assessed with the SPSS GLM routine.

Results

The interaction between Kir6.1/SUR2B channels and caveolin inhibits channel activity

To assess the possible functional implications of the interaction between caveolin and K_{ATP} channels, whole-cell recombinant Kir6.1/SUR2B currents were recorded from caveolin-null HEK293 (HEK293) and HEK293 stably expressing caveolin-1 (HEK293 caveolin-1). Pinacidil-evoked, glibenclamide-sensitive whole-cell Kir6.1/SUR2B currents recorded at a holding potential of −60 mV were significantly smaller in HEK293 cells stably expressing caveolin-1 (69.6 ± 8.3 pA pF^{-1}, $n = 8$; Fig. 1*B* and *C*) than in caveolin-null cells (179.7 ± 35.9 pA pF^{-1}, $n = 6$; $P < 0.05$; Fig. 1*A* and *C*). Cell size as measured using whole-cell capacitance was unaffected by the presence of caveolin (HEK293: 8.3 ± 3.4 pF, $n = 6$; HEK293 caveolin-1: 8.1 ± 1.4 pF, $n = 8$). Since changes in whole-cell current amplitude may reflect differences in channel subunit expression between caveolin-null cells and cells stably expressing caveolin-1, we tested the effects of including a peptide corresponding to the caveolin-1 scaffolding domain (residues 82–101; 10 μM) in the pipette-filling solution. Inclusion of the caveolin-1 scaffolding domain peptide

(SDP) in the pipette-filling solution had a similar effect on pinacidil-evoked whole-cell Kir6.1/SUR2B currents recorded in caveolin-null cells as co-expression with full-length caveolin-1 (Fig. 1*D*). Inclusion of a scrambled version of this peptide (10 μM) in the pipette-filling solution did not significantly alter whole-cell currents.

To investigate whether this caveolin-induced reduction in whole-cell Kir6.1/SUR2B currents resulted from a change in the sensitivity of the channel to pinacidil, we

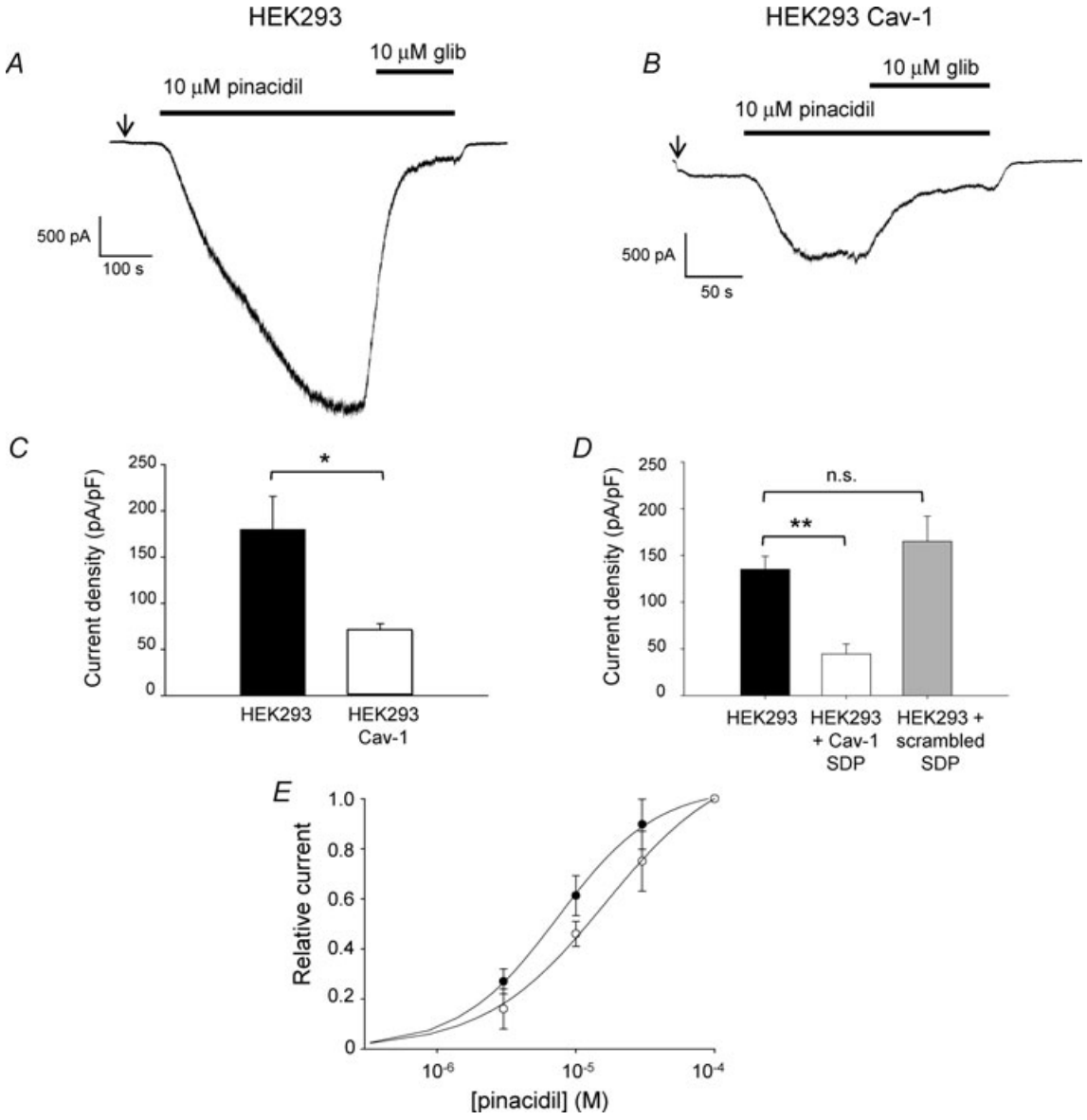

Figure 1. The presence of caveolin-1 reduces whole-cell recombinant Kir6.1/SUR2B currents
A and *B*, representative pinacidil-evoked whole-cell Kir6.1/SUR2B currents recorded at −60 mV in 140 mM K^+ from caveolin-null HEK293 (*A*) or a HEK293 cell line stably expressing caveolin-1 (*B*). The vascular K_{ATP} channel activator pinacidil (10 μM) and the specific K_{ATP} channel blocker glibenclamide (10 μM) were applied as indicated. The arrow indicates the extracellular solution was changed from 6 mM to 140 mM K^+ to increase the inward driving force for K^+. *C*, mean amplitude of glibenclamide-sensitive current in experiments like those in *A* and *B* (means ± S.E.M., $n = 6$, 8 cells, $^*P < 0.05$). *D*, mean amplitude of glibenclamide-sensitive current in caveolin-null HEK293 cells in response to inclusion of caveolin-1 scaffolding domain peptide (SDP; 10 μM) or a scrambled version of this peptide (10 μM) in the pipette-filling solution (means ± S.E.M., $n = 12$, 6, 4 cells, $^{**}P < 0.01$; n.s., not significant). The caveolin-1 SDP or the scrambled version of this peptide was allowed to dialyse into the cell for 10 min prior to the start of recording. *E*, response of caveolin-null HEK293 cells (filled symbols) or HEK293 cell line stably expressing caveolin-1 (open symbols) to different concentrations of pinacidil (3–100 μM; means ± S.E.M., $n = 4$, 3 cells, not significant).

obtained dose–response curves over the range 3–100 μM in the presence and absence of caveolin-1. Figure 1*E* shows that the channel's response to pinacidil is not significantly altered by the presence of caveolin-1.

We also investigated the effects of the caveolin SDP on native whole-cell K_{ATP} currents recorded from single isolated rat aortic smooth muscle cells. We hypothesised that dialysis of the SDP into the cell would uncouple constitutive K_{ATP}–caveolin complexes leading to an increase in whole-cell current amplitude. Interestingly, inclusion of the caveolin-1 SDP in the pipette-filling solution had the opposite effect, causing a significant inhibition of pinacidil-evoked whole-cell K_{ATP} currents (control: 20.4 ± 1.0 pA pF^{-1}, $n = 6$; +SDP: 9.2 ± 1.9 pA pF^{-1}, $n = 6$; $P < 0.05$; Fig. 2*A*–*C*). Intracellular dialysis of the cell with the scrambled version of the peptide did not alter whole-cell current amplitude (Fig. 2*C*), suggesting that this was not a non-specific effect of the presence of peptide within the cell.

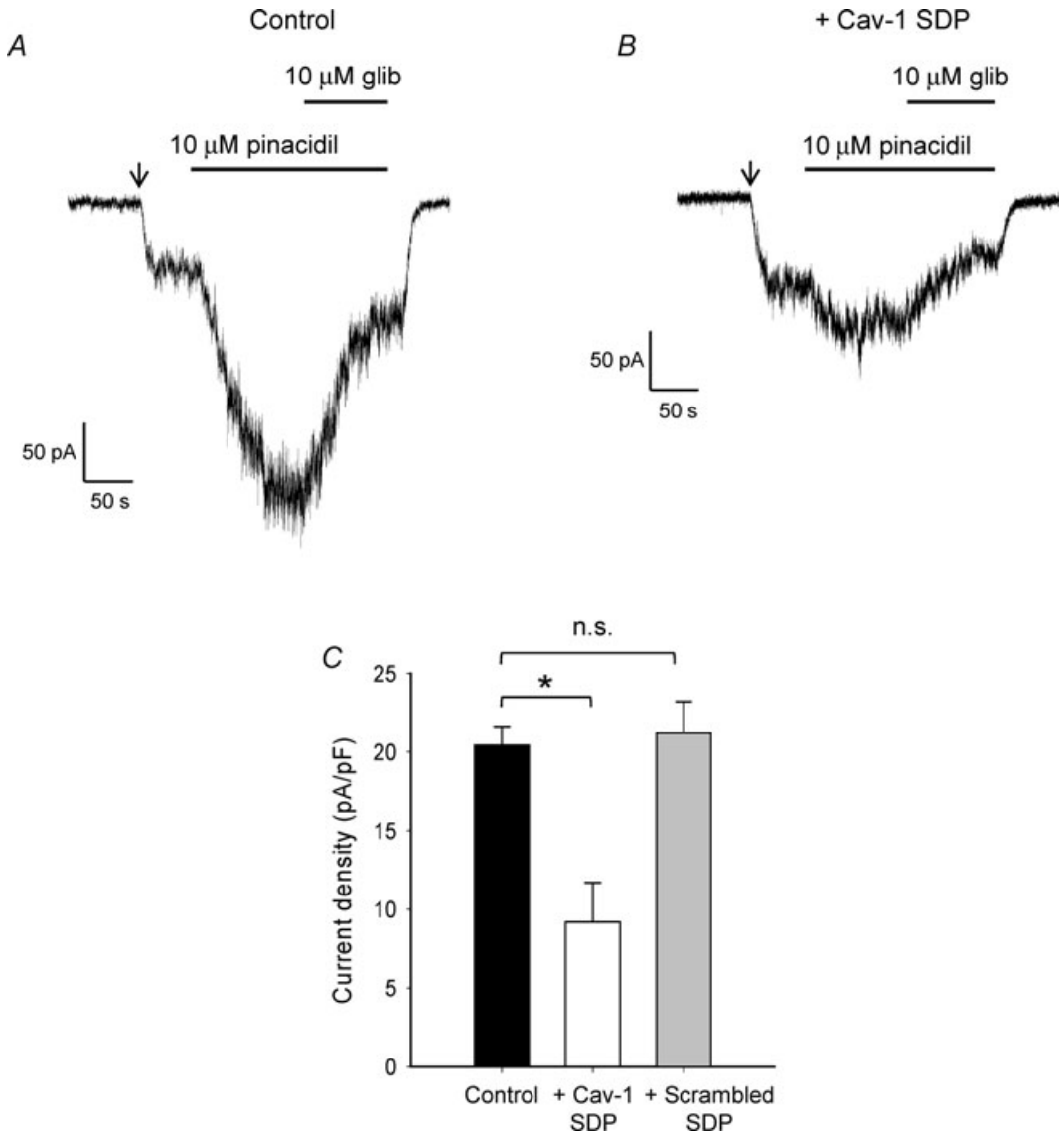

Figure 2. Inclusion of the caveolin-1 scaffolding domain peptide in the pipette-filling solution reduces whole-cell K_{ATP} current in aortic smooth muscle cells
A and *B*, whole-cell current recorded from single isolated rat aortic smooth muscle cells at −60 mV under control conditions (*A*) or with the inclusion of the caveolin-1 scaffolding domain peptide (SDP; 10 μM) in the pipette-filling solution (*B*). The arrow indicates the extracellular solution was changed from 6 mM to 140 mM K^+ to increase the inward driving force for K^+. *C*, mean amplitude of glibenclamide-sensitive current in response to inclusion of caveolin-1 scaffolding domain peptide (SDP; 10 μM) or a scrambled version of this peptide (10 μM) in the pipette-filling solution (means ± S.E.M., $n = 6$, 6, 4 cells, $^*P < 0.05$; n.s., not significant). The caveolin-1 SDP or the scrambled peptide was allowed to dialyse into the cell for 10 min prior to the start of recording.

A reduction in whole-cell current in the presence of caveolin may reflect a change in the number of functional channels at the cell surface, a reduction in the single channel conductance, or a change in channel kinetics resulting in the channel spending less time open. To distinguish between these possibilities, cell-attached recordings were made of single Kir6.1/SUR2B channels in HEK293 cells in the presence and absence of caveolin. Bath application of 10 μM pinacidil to cells transiently transfected with cDNAs encoding Kir6.1/SUR2B induced the opening of K^+ channels with a unitary amplitude of ~2 pA at −60 mV that were blocked by exposure to glibenclamide. No channel openings were observed in response to pinacidil in non-transfected cells. The kinetics of the pinacidil-activated, glibenclamide-sensitive channels were characterised by bursts of rapid openings and closings, separated by long closures (Fig. 3*A* and *B*). This behaviour is consistent with native vascular-type K_{ATP} channels (Beech *et al.* 1993*a*,*b*; Zhang & Bolton, 1996).

Analysis of single channel conductance over a range of different potentials revealed no significant change in the presence of caveolin. Single-channel conductance was calculated at −80 mV to be 39.7 ± 2.1 pS for caveolin-null HEK293 cells and 35.0 ± 2.8 pS for HEK293 caveolin-1 cells. This is within the conductance range (20–40 pS) reported for K_{ATP} channels in vascular smooth muscle cells (Cole & Clement-Chomienne, 2003).

While recording single K_{ATP} channel activity from caveolin-containing HEK293 cells it became evident that the channels appeared to be less active than those recorded from caveolin-null cells (representative traces shown in Fig. 3*A*, *B*). Notably, burst lengths were greatly reduced from 42 ± 8 ms in caveolin-null cells to 3.8 ± 1.5 ms in cells co-expressing caveolin-1 ($n = 7$, $P < 0.05$). This was reflected in a significant reduction in the open probability of pinacidil-evoked channels recorded in cells containing caveolin (Fig. 3*D*; 0.05 ± 0.01 to 0.005 ± 0.001, $P < 0.05$).

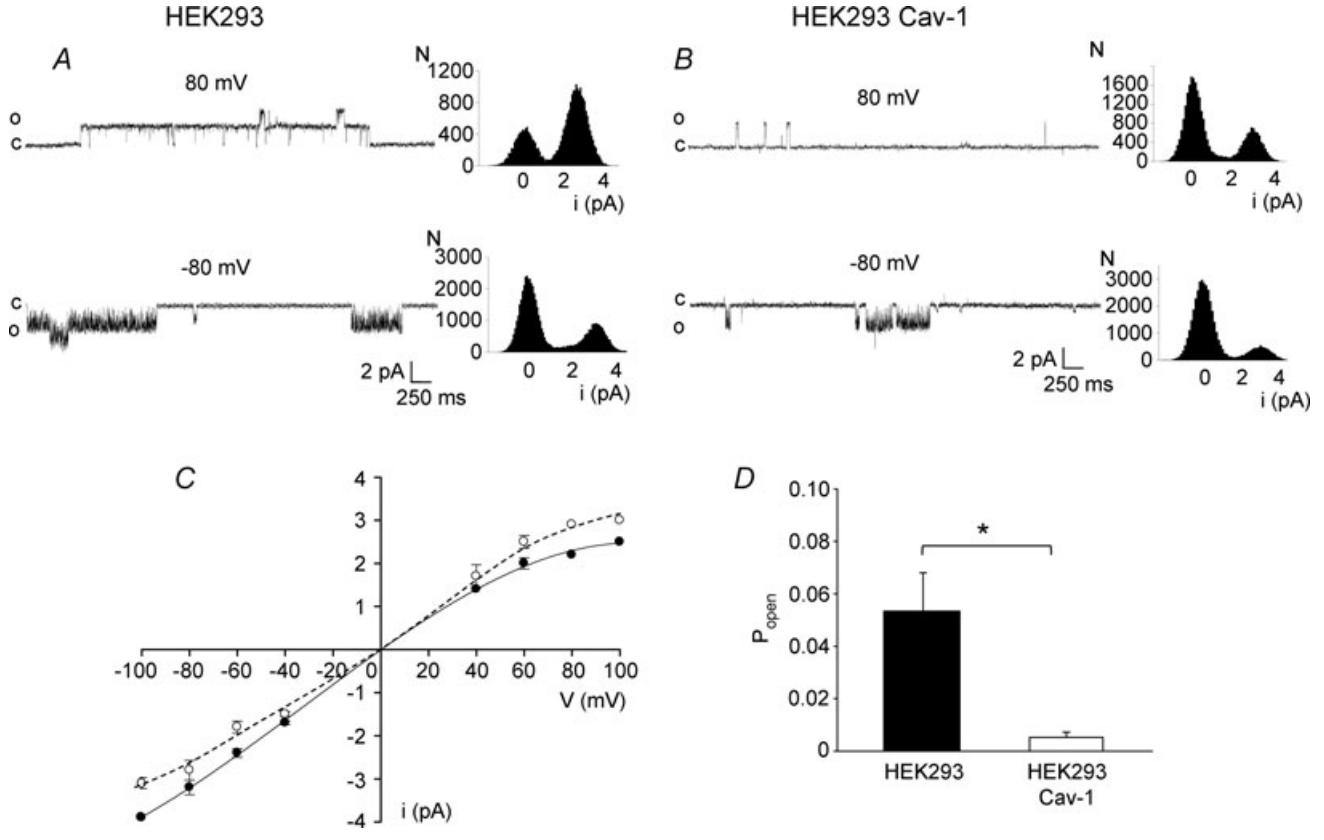

Figure 3. Single channel conductance is unaffected by the presence of caveolin
A and *B*, single-channel Kir6.1/SUR2B currents recorded at membrane potentials of 80 mV and −80 mV from cell-attached patches from caveolin-null HEK293 cells (*A*) or HEK293 cells stably expressing caveolin-1 (*B*). Currents were recorded in 140 mM extracellular K^+ and 10 μM pinacidil. All-point amplitude histograms shown on the right of each trace. *C*, mean single channel amplitudes for Kir6.1/SUR2B channels expressed in caveolin-null HEK293 cells (filled symbols) or HEK293-caveolin-1 cells (open symbols) plotted against voltage (means ± S.E.M.). *D*, open probability of pinacidil-evoked Kir6.1/SUR2B channels recorded in caveolin-null HEK293 or HEK293 caveolin-1 cells at −40 mV (*$P < 0.05$).

Single channel model

To further explore the complex kinetic behaviour of Kir6.1/SUR2B channels, we idealized single channel recordings from caveolin-null and caveolin-1 containing HEK293 cells using the segmental K means (SKM) methods (Qin, 2004) (Fig. 4*A*). We then constructed the simplest stoichometric models which could accurately describe the SKM minimised dwell time data. We increased the numbers of states progressively and for each of these performed a 'model search' procedure which trialled all the possible interconnections between states (see Methods). Following examination of several hundred such models, the schema in Fig. 4*B* returned the overall highest aggregate log-likelihood/event for all our combined caveolin-null and caveolin-1 cell data. This model has two open states (O1, O2) and three closed states (C1, C2, C3). C1 represents the long-lived closed state between bursts of activity, and the rapid openings and closures seen within these bursts can be explained by transitions between the remaining states. The mean rate constants for transitions between all states in the model are shown in Table 1. The presence of caveolin significantly increases the number of times per second that the channel transits from O2 to long-lived C1 (rate 2 in Table 1; $P < 0.05$) and significantly decreases the number of times per second that the channel transits from O2 to O1 (rate 8 in Table 1; $P < 0.05$). These changes in rate constant will affect the relative amount of time a channel spends in each of the states. This is reflected in the mean equilibrium occupancy data (Table 2), which indicates that in the presence of caveolin, channels spend significantly less time in open-state O1. Figure 5 shows the dwell time histograms for Kir6.1/SUR2B channels recorded in the presence and absence of caveolin-1. The probability distribution functions computed for this five-state model are shown superimposed over each histogram.

Table 1. Mean rate constants for transitions between states in the model

	Rate constant (s^{-1})	
Rate	HEK293	HEK293 Cav-1
1	0.37 ± 0.08	0.68 ± 0.35
2	286 ± 13	1256 ± 81*
3	148 ± 23	255 ± 90
4	811 ± 57	946 ± 388
5	5144 ± 2096	2528 ± 58
6	2395 ± 1458	467 ± 54
7	37 ± 8.6	45 ± 2.6
8	1856 ± 289	718 ± 49*

Interaction with caveolin alters K_{ATP} channel sensitivity to MgADP

A possible mechanism by which interaction with caveolin could suppress K_{ATP} channel openings is by altering the channel's sensitivity to physiological regulators. Vascular K_{ATP} channels are characterised by their relative insensitivity to changes in intracellular ATP and, unlike pancreatic and cardiac K_{ATP} channels, do not open spontaneously when ATP is absent. Instead they require the presence of di- or tri-nucleotides and magnesium on the cytoplasmic face of the membrane before they gate (Beech *et al.* 1993*a*,*b*; Zhang & Bolton, 1996). Di- or tri-nucleotides thus activate the channel, although at high concentrations have an inhibitory effect leading to a characteristic bell-shaped concentration–response curve (Zhang & Bolton, 1996). It has been suggested that net activity of the channel is the product of nucleotide-mediated activation and inhibition, although the molecular basis of these mechanisms has not been fully elucidated for the vascular channel.

To address the possibility that interaction with caveolin alters the Kir6.1/SUR2B channel's response to nucleotides,

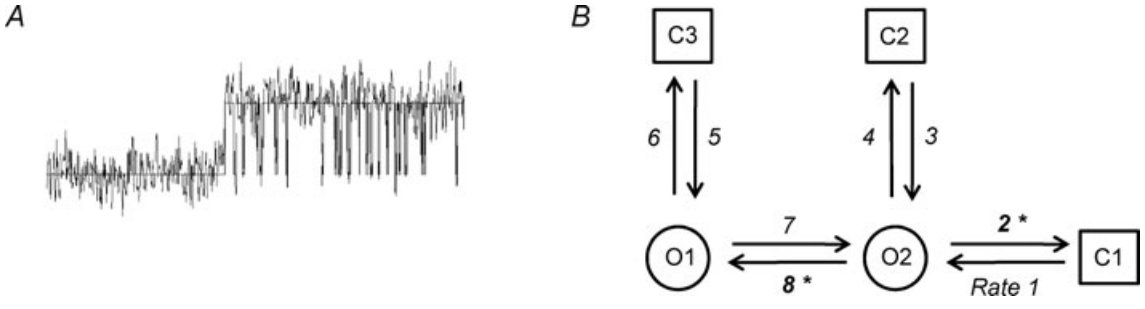

Figure 4. Model of single Kir6.1/SUR2B channel behaviour
A, segment of single channel recording superimposed with SKM idealized trace. *B*, schema showing the possible relationship between the different open and closed states. The model illustrated represents that with the greatest aggregate log-likelihood/event value of the several hundred models searched with the constraints of requiring a minimum number of states, a maximum of 8 transitions and 3 exits per state.

Table 2. Mean equilibrium occupancy for six patches for each state of the model

	Equilibrium occupancy	
State	HEK293	HEK293 Cav-1
C1	0.91 ± 0.04	0.97 ± 0.03
O1	0.06 ± 0.02	0.007 ± 0.006*
C2	0.006 ± 0.001	0.018 ± 0.03
O2	0.0012 ± 0.0004	0.0005 ± 0.0004
C3	0.025 ± 0.02	0.0011 ± 0.0006

inside-out patches were recorded from caveolin-null HEK293 and HEK293 caveolin-1 cells at differing concentrations of the adenine nucleotides ATP and ADP. Activation of the recombinant vascular K_{ATP} channel by ATP in the presence of Mg^{2+} was concentration dependent (Fig. 6*A*). Maximum channel activation was seen in both caveolin-null HEK293 and HEK293 caveolin-1 at concentrations around 1 mM ATP, consistent with previous findings (Satoh *et al.* 1998). At concentrations above 1 mM, ATP was less effective at activating Kir6.1/SUR2B channels in both HEK293 and HEK293 caveolin-1 cells, producing a bell-shaped concentration–response curve. When fitted with a biphasic concentration effect curve (see eqn (1), Methods), there was no significant change in either K_{d1} or K_{d2} in patches pulled from caveolin-null and caveolin-1 expressing cells (HEK293: K_{d1} $103 \pm 29\,\mu$M, K_{d2} 1.6 ± 0.8 mM; HEK293 Cav-1: K_{d1} $144 \pm 13\,\mu$M, K_{d2} 1.5 ± 0.3 mM, $n = 9$, $P > 0.05$). This suggests that the presence of caveolin-1 did not significantly affect the sensitivity of the Kir6.1/SUR2B channel to MgATP over the range tested.

Application of 10 μM ADP in the presence of Mg^{2+} activated recombinant Kir6.1/SUR2B channels in patches

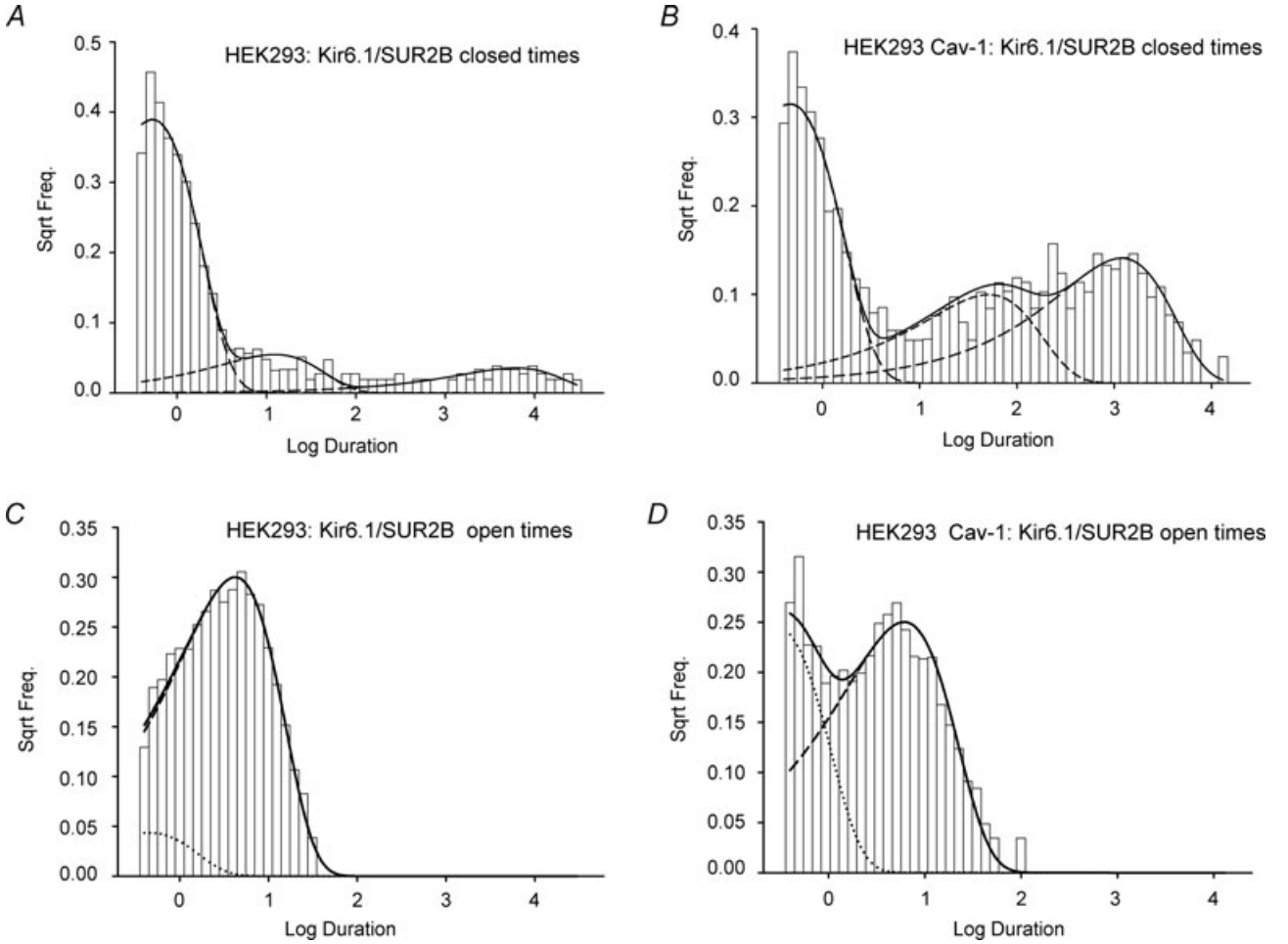

Figure 5. Caveolin induces changes in state occupancy
Open and closed dwell time distributions measured in cell-attached patch mode at −40 mV for caveolin-null HEK293 cells (*A* and *C*) or HEK293 caveolin-1 cells (*B* and *D*) expressing Kir6.1/SUR2B. Continuous lines show the probability distribution function directly computed from the schemas illustrated in Fig. 4. Dashed lines represent the individual component exponentials (2 open, 3 closed), each computed from the schema's Q matrix inverse eigenvalues.

excised from both HEK293 and HEK293 caveolin-1 cells (Fig. 6*B*–*D*). At this concentration, activation was significantly higher in HEK293 caveolin-1 cells ($P < 0.01$). For caveolin-null HEK293 cells maximum activation by ADP occurred at 1 mM, with concentrations above this being less effective at sustaining activation. In contrast, maximum activation in HEK293 caveolin-1 cells occurred at the lower concentration of 100 μM, with concentrations above this decreasing the level of activation and producing a significant leftward shift in the concentration–response curve (Fig. 6*B*, HEK293: K_{d1} 96 ± 9 μM, K_{d2} 1.9 ± 0.1 mM. HEK293 Cav-1: K_{d1} 16 ± 1 μM, K_{d2} 0.7 ± 0.2 mM, $n = 10$, $P < 0.005$). This means that over the physiological intracellular ADP concentration range (~100 μM to 1 mM; Clark *et al.* 1995; Innocenti *et al.* 1996; Yoon *et al.* 2001), MgADP is less effective at activating the channel in the presence of caveolin-1.

Discussion

Our findings suggest that interaction between vascular-type K_{ATP} channels and the cholesterol-binding protein caveolin results in a marked reduction in channel activity. The complex kinetic behaviour of the Kir6.1/SUR2B channel, characterised by bursts of rapid openings and closings separated by long closures, is most simply described by a model in which the channel has two distinct open states (O1, O2) and three distinct closed states (C1, C2, C3). In this model, C1 represents the long-lived closed state and rapid transitions between the remaining states can be used to explain bursting activity. The presence of caveolin alters the rates at which the channel transits between these states, significantly decreasing the number of times per second that the channel transits between the two open states and

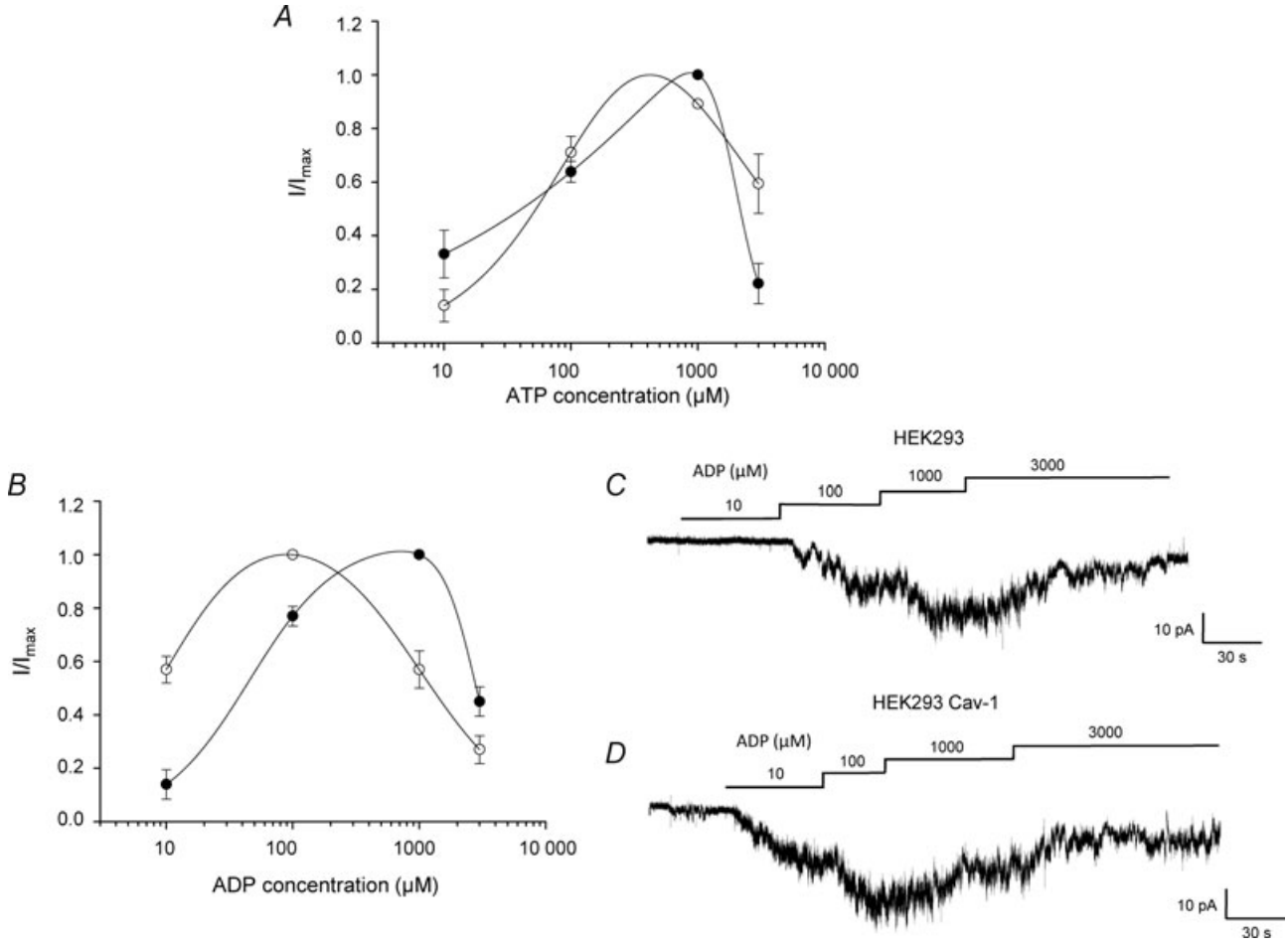

Figure 6. Caveolin alters vascular K_{ATP} channel sensitivity to MgADP
A and *B*, concentration–response relationship of the ATP-induced (*A*) or ADP-induced (*B*) activation of recombinant Kir6.1/SUR2B channels in the presence 10 μM pinacidil for both caveolin-null HEK293 (filled symbols) and HEK293 caveolin-1 (open symbols) cells (means ± S.E.M., $n = 6$, 6 patches respectively). Channels were recorded in inside out patches at −60 mV. Data are fitted with a biphasic concentration–effect curve (see eqn (1); Methods). *C* and *D*, ADP-induced concentration-dependent activation of recombinant vascular K_{ATP} channels in inside-out patches pulled from caveolin-null HEK293 cells (*C*) and HEK293 cells stably expressing caveolin-1 (*D*).

significantly increasing the number of times per second that the channel transits out of O2 into long-lived closed state C1. This would account for the significant reduction in burst length seen in the presence of caveolin and the overall reduction in channel open probability.

A possible explanation for these changes in kinetic behaviour is provided by the finding that interaction with caveolin-1 causes a shift the channel's sensitivity to its physiological regulator MgADP. Due to the bell shape of the MgADP concentration–response curve this means that under our recording conditions intracellular levels of ADP greater than $\sim 200\ \mu$M would be expected to be less effective at activating K_{ATP} channels in the presence of caveolin. This equates to the conditions we used in both our cell-attached and whole-cell experiments and may account for the significant caveolin-induced reduction in activity seen in these experiments. Nucleotide activation of K_{ATP} channels in the presence of magnesium involves binding of ATP or ADP to two large intracellular loops on the channel's modulatory SUR subunit that contain consensus sequences for nucleotide binding and hydrolysis (Aguilar-Bryan *et al.* 1998; Aguilar-Bryan & Bryan, 1999; Seino, 1999). The interaction between caveolin and the K_{ATP} channel also most likely occurs through interaction between the caveolin scaffolding domain (CSD) and specific targeting residues on the SUR2B subunits. Involvement of the CSD in the interaction is supported by the fact that dialysis of caveolin-null HEK293 cells with a 20 amino acid peptide equivalent to the CSD sequence on caveolin-1 had a similar effect on whole cell K_{ATP} currents as co-expression with full length caveolin-1. The CSD is known to bind to specific sequences on target proteins (ΦXΦXXXXΦ, ΦXXXXΦXXΦ and ΦXΦXXXXΦXXΦ where Φ is an aromatic amino acid Trp, Phe or Tyr) (Couet *et al.* 1997; Patel *et al.* 2008). None of these caveolin targeting sequences appear on the pore-forming Kir6.1 subunit; however, the sequence ΦXΦXXXXΦ appears twice on SUR2B, at positions 138–145 (FLYWVMAF) and 1142–1149 (FYFIQKYF). Precisely how interaction with caveolin affects SUR2B function, particularly in relation to MgADP binding and activation, and whether this occurs as a regulatory mechanism within the vasculature await further investigation. Recent studies also suggest that activation of protein kinase Cε (PKCε) induces the caveolin-dependent internalization of K_{ATP} channels (Jiao *et al.* 2008). While our findings indicate that association between caveolin-1 and Kir6.1/SUR2B causes significant changes in kinetic behaviour at a single channel level, our work does not exclude the possibility that interaction with caveolin might also alter the functional number of channels at the cell surface.

A particularly striking finding of this study is that intracellular dialysis of vascular smooth muscle cells with the caveolin-1 SDP causes a significant inhibition of whole-cell K_{ATP} current. A possible explanation for our finding is that within vascular cells a significant proportion of native K_{ATP} channels remain unassociated with caveolin and are thus available and susceptible to block by exogenously applied SDP. This would be in agreement with membrane fractionation data from vascular tissue which show a population of K_{ATP} channels in cholesterol-enriched membrane fractions that do not label for caveolin (Sampson *et al.* 2007). Whether these membrane fractions represent non-caveolae forms of lipid rafts remains unclear as is the relationship between these different K_{ATP} channel populations.

A potential link between caveolins and K_{ATP} channels is interesting in the context of both normal channel physiology and in the pathophysiology of certain disease states. Of particular interest is the fact that caveolin expression is regulated by the free cholesterol content within cells, with caveolin mRNA and protein levels both increased in cells exposed to low-density lipoprotein (LDL), a major cholesterol-rich plasma lipoprotein (Fielding *et al.* 1997; Hailstones *et al.* 1998). A number of functional studies show that reduced membrane cholesterol decreases vascular responses, while hypercholesterolaemia increases vascular reactivity to certain vasoconstrictor hormones (Merkel & Bilder, 1992; Mathew *et al.* 1997; Romerio *et al.* 2000). Physiologically, the tonic background activity of vascular K_{ATP} channels has been implicated in maintaining a vasodilating drive to resting vascular tone (Samaha *et al.* 1992; Moreau *et al.* 1994; Farouque *et al.* 2000). This is emphasised by the fact that loss of vascular K_{ATP} channel subunits in transgenic mice leads to arterial hypercontractility and hypertension (Chutkow *et al.* 2002; Miki *et al.* 2002). Elevated levels of free cholesterol and increased caveolin expression may thus have the effect of 'silencing' populations of K_{ATP} channels, which may be an important contributory factor to the pathophysiological changes in vascular contractility.

References

Aguilar-Bryan L & Bryan J (1999). Molecular biology of adenosine triphosphate-sensitive potassium channels. *Endocr Rev* **20**, 101–135.

Aguilar-Bryan L, Clement JP, Gonzalez G, Kunjilwar K, Babenko A & Bryan J (1998). Toward understanding the assembly and structure of K-ATP channels. *Physiol Rev* **78**, 227–245.

Anderson RGW (1998). The caveolae membrane system. *Annu Rev Biochem* **67**, 199–225.

Barrett-Jolley R, Dart C & Standen NB (1999). Direct block of native and cloned (Kir2.1) inward rectifier K^+ channels by chloroethylclonidine. *Brit J Pharmacol* **128**, 760–766.

Beech DJ, Zhang H, Nakao K & Bolton TB (1993*a*). K channel activation by nucleotide diphosphates and its inhibition by glibenclamide in vascular smooth muscle cells. *Br J Pharmacol* **110**, 573–582.

Beech DJ, Zhang H, Nakao K & Bolton TB (1993*b*). Single channel and whole-cell K currents evoked by levcromakalim in smooth muscle cells from the rabbit portal vein. *Br J Pharmacol* **110**, 583–590.

Chutkow WA, Pu JL, Wheeler MT, Wada T, Makielski JC, Burant CF & McNally EM (2002). Episodic coronary artery vasospasm and hypertension develop in the absence of Sur2 K-ATP channels. *J Clin Invest* **110**, 203–208.

Clapp LH & Tinker A (1998). Potassium channels in the vasculature. *Curr Opin Nephrol Hypertens* **7**, 91–98.

Clark JF, Kemp GJ & Radda GK (1995). The creatine-kinase equilibrium, free [ADP] and myosin ATPase in vascular smooth muscle cross bridges. *J Theor Biol* **173**, 207–211.

Cole WC & Clement-Chomienne O (2003). ATP-sensitive K^+ channels of vascular smooth muscle cells. *J Cardiovasc Electrophysiol* **14**, 94–103.

Couet J, Li SW, Okamoto T, Ikezu T & Lisanti MP (1997). Identification of peptide and protein ligands for the caveolin-scaffolding domain: Implications for the interaction of caveolin with caveolae-associated proteins. *J Biol Chem* **272**, 6525–6533.

Farouque HMO, Worthley SG, Meredith IT, Skyrme-Jones PAP & Zhang MJ (2000). Effect of ATP-sensitive potassium channel inhibition on resting coronary vascular responses in humans. In *73rd Scientific Sessions of the American Heart Association*, pp. 231–236.

Fielding CJ, Bist A & Fielding PE (1997). Caveolin mRNA levels are up-regulated by free cholesterol and down-regulated by oxysterols in fibroblast monolayers. *Proc Natl Acad Sci U S A* **94**, 3753–3758.

Galbiati F, Razani B & Lisanti MP (2001). Emerging themes in lipid rafts and caveolae. *Cell* **106**, 403–411.

Garg V, Jiao JD & Hu KL (2009*a*). Regulation of ATP-sensitive K^+ channels by caveolin-enriched microdomains in cardiac myocytes. *Cardiovasc Res* **82**, 51–58.

Garg V, Sun W & Hu KL (2009*b*). Caveolin-3 negatively regulates recombinant cardiac K-ATP channels. *Biochem Biophys Res Commun* **385**, 472–477.

Hailstones D, Sleer LS, Parton RG & Stanley KK (1998). Regulation of caveolin and caveolae by cholesterol in MDCK cells. *J Lipid Res* **39**, 369–379.

Innocenti B, Pozzan T & Fasolato C (1996). Intracellular ADP modulates the Ca^{2+} release-activated Ca^{2+} current in a temperature- and Ca^{2+}-dependent way. *J Biol Chem* **271**, 8582–8587.

Jiao JD, Garg V, Yang BF, Elton TS & Hu KL (2008). Protein kinase C-ε induces caveolin-dependent internalization of vascular adenosine 5′-triphosphate sensitive K^+ channels. *Hypertension* **52**, 499–506.

Leyland ML & Dart C (2004). An alternatively spliced isoform of PSD93/Chapsyn 110 binds to the inwardly rectifying potassium channel, Kir2.1. *J Biol Chem* **279**, 43427–43436.

Mathew V, Cannan CR, Miller VM, Barber DA, Hasdai D, Schwartz RS, Holmes DR & Lerman A (1997). Enhanced endothelin-mediated coronary vasoconstriction and attenuated basal nitric oxide activity in experimental hypercholesterolemia. *Circulation* **96**, 1930–1936.

Merkel LA & Bilder GE (1992). Modulation of vascular reactivity by vasoactive peptides in aortic rings from hypercholesterolemic rabbits. *Eur J Pharmacol* **222**, 175–179.

Miki T, Suzuki M, Shibasaki T, Uemura H, Sato T, Yamaguchi K, Koseki H, Iwanaga T, Nakaya H & Seino S (2002). Mouse model of Prinzmetal angina by disruption of the inward rectifier Kir6.1. *Nat Med* **8**, 466–472.

Moreau R, Komeichi H, Kirstetter P, Yang S, Aupetitfaisant B, Cailmail S & Lebrec D (1994). Effects of glibenclamide on systemic and splanchnic hemodynamics in conscious rats. *Br J Pharmacol* **112**, 649–653.

Okamoto T, Schlegel A, Scherer PE & Lisanti MP (1998). Caveolins, a family of scaffolding proteins for organizing "preassembled signaling complexes" at the plasma membrane. *J Biol Chem* **273**, 5419–5422.

Parton RG & Simons K (2007). The multiple faces of caveolae. *Nat Rev Mol Cell Biol* **8**, 185–194.

Patel HH, Murray F & Insel PA (2008). Caveolae as organizers of pharmacologically relevant signal transduction molecules. *Annu Rev Pharmacol Toxicol* **48**, 359–391.

Qin F (2004). Restoration of single-channel currents using the segmental k-means method based on hidden Markov modeling. *Biophys J* **86**, 1488–1501.

Qin F, Auerbach A & Sachs F (1996). Estimating single-channel kinetic parameters from idealized patch-clamp data containing missed events. *Biophys J* **70**, 264–280.

Qin F, Auerbach A & Sachs F (1997). Maximum likelihood estimation of aggregated Markov processes. *Proc R Soc Lond B Biol Sci* **264**, 375–383.

Quayle JM, Nelson MT & Standen NB (1997). ATP-sensitive and inwardly rectifying potassium channels in smooth muscle. *Physiol Rev* **77**, 1165–1232.

Razani B, Woodman SE & Lisanti MP (2002). Caveolae: From cell biology to animal physiology. *Pharmacol Rev* **54**, 431–467.

Romerio SC, Linder L, Flammer J & Haefeli WE (2000). Correlation between apolipoprotein B and endothelin-1-induced vasoconstriction in humans. *Peptides* **21**, 871–874.

Samaha FF, Heineman FW, Ince C, Fleming J & Balaban RS (1992). ATP-sensitive potassium channel is essential to maintain basal coronary vascular tone in vivo. *Am J Physiol Cell Physiol* **262**, C1220–C1227.

Sampson LJ, Davies LM, Barrett-Jolley R, Standen NB & Dart C (2007). Angiotensin II-activated protein kinase C targets caveolae to inhibit aortic ATP-sensitive potassium channels. *Cardiovasc Res* **76**, 61–70.

Sampson LJ, Hayabuchi Y, Standen NB & Dart C (2004). Caveolae localize protein kinase A signaling to arterial ATP-sensitive potassium channels. *Circ Res* **95**, 1012–1018.

Satoh E, Yamada M, Kondo C, Repunte VP, Horio Y, Iijima T & Kurachi Y (1998). Intracellular nucleotide-mediated gating of SUR/Kir6.0 complex potassium channels expressed in a mammalian cell line and its modification by pinacidil. *J Physiol* **511**, 663–674.

Seino S (1999). ATP-sensitive potassium channels: A model of heteromultimeric potassium channel/receptor assemblies. *Annu Rev Physiol* **61**, 337–362.

Yokoshiki H, Sunagawa M, Seki T & Sperelakis N (1998). ATP-sensitive K^+ channels in pancreatic, cardiac, and vascular smooth muscle cells. *Am J Physiol Cell Physiol* **43**, C25–C37.

Yoon HY, Hwang SH, Lee EY, Kim TU, Cho EH & Cho SW (2001). Effects of ADP on different inhibitory properties of brain glutamate dehydrogenase isoproteins by perphenazine. *Biochimie* **83**, 907–913.

Zhang HL & Bolton TB (1996). Two types of ATP-sensitive potassium channels in rat portal vein smooth muscle cells. *Br J Pharmacol* **118**, 105–114.

Author contributions

L.M.D.: all experiments, conception and design of experiments, analysis and interpretation of data, drafting the article and revising it critically for important intellectual content, and final approval of the version to be published. G.I.P.: analysis and interpretation of data, drafting the article and revising it critically for important intellectual content and final approval of the version to be published. R.B.-J.: model of single Kir6.1/SUR2B channel behaviour, analysis and interpretation of data, drafting the article and revising it critically for important intellectual content and final approval of the version to be published. C.D.: conception and design of experiments, analysis and interpretation of data, drafting the article and revising it critically for important intellectual content, and final approval of the version to be published. Experiments were undertaken in the School of Biological Sciences at the University of Liverpool.

Acknowledgements

We thank the Biotechnology and Biological Sciences Research Council and the British Heart Foundation for their support.